Synthesis of Poly(aniline-*co*-*o*-toluidine) Coatings and Their Corrosion-Protection Performance on Low-Carbon Steel

Pritee Pawar,[1] S. R. Sainkar,[2] P. P. Patil[1]

[1]*Department of Physics, North Maharashtra University, Jalgaon 425 001, Maharashtra, India*
[2]*Center for Materials Characterization, National Chemical Laboratory, Pashan, Pune 411 008, Maharashtra, India*

Received 15 February 2006; accepted 20 August 2006
DOI 10.1002/app.25346
Published online in Wiley InterScience (www.interscience.wiley.com).

ABSTRACT: Strongly adherent poly(aniline-*co*-*o*-toluidine) coatings were synthesized on low-carbon-steel substrates by the electrochemical copolymerization of aniline with *o*-toluidine with sodium tartrate as the supporting electrolyte. These coatings were characterized with cyclic voltammetry, ultraviolet–visible absorption spectroscopy, Fourier transform infrared spectroscopy, nuclear magnetic resonance spectroscopy, and scanning electron microscopy. The formation of the copolymer with the mixture of monomers in the aqueous sodium tartrate solution was ascertained by a critical comparison of the results obtained from the polymerizations of the individual monomers, aniline and *o*-toluidine. The optical absorption spectrum of the copolymer was drastically different from the spectra of the respective homopolymers, polyaniline and poly(*o*-toluidine). The extent of the corrosion protection offered by poly(aniline-*co*-*o*-toluidine) coatings to low-carbon steel was investigated in aqueous 3% NaCl solutions by open-circuit-potential measurements and a potentiodynamic polarization technique. The results of the potentiodynamic polarization measurements showed that the poly(aniline-*co*-*o*-toluidine) coatings provided more effective corrosion protection to low-carbon steel than the respective homopolymers. The corrosion rate depended on the feed ratio of *o*-toluidine used for the synthesis of the copolymer coatings. © 2006 Wiley Periodicals, Inc. J Appl Polym Sci 103: 1868–1878, 2007

Key words: coatings; conducting polymers; copolymerization; synthesis

INTRODUCTION

During last 2 decades and even now, conducting polymers continue to be the focus of active research in many technological areas, such as rechargeable batteries,[1,2] sensors,[3,4] electromagnetic interference shielding,[5,6] electrochromic display devices,[7,8] smart windows,[9] molecular devices,[10] energy-storage systems,[11] and membrane gas separation,[12] because of their remarkable physical attributes. The use of conducting polymers as advanced coating materials for the corrosion protection of oxidizable metals has become one of the most exciting new research fields in recent times.[13–19] Mengoli et al.[20] were the first to examine the protective behavior of polyaniline (PANI) on stainless steel, and then in 1985, DeBerry[21] showed that electrochemically synthesized PANI acts as a corrosion-protection layer on stainless steel in 1*M* H_2SO_4. Since then, several research groups[22–26] have systematically investigated the electrochemical syntheses of various conducting polymers on oxidizable metals for corrosion protection. The common feature of these investigations is that the electrochemical synthesis of conducting polymer coatings on oxidizable metals is preceded by the dissolution of the base metal at a potential lower than the oxidation potential of the monomer. Thus, the oxidation of the metal appears as a simultaneous and competitive oxidation process at potentials adequate for the formation of the polymer. Hence, a successful electrochemical synthesis of conducting polymer coatings on oxidizable metals demands a careful choice of the solvent and/or supporting electrolyte and the establishment of electrochemical parameters that will strongly passivate the metal without impeding the electropolymerization process.

Among the conducting polymers, PANI and polypyrrole are the most promising conducting polymers for the corrosion protection of metals. The extent of the use of these conducting polymers is limited by the exclusivity of the monomers that are essential for their synthesis.[27,28] To overcome this limitation, different synthesis approaches have been attempted.

Correspondence to: P. P. Patil (pnmu@yahoo.co.in).
Contract grant sponsor: University Grants Commission (New Delhi, India; through the SAP–DRS program).
Contract grant sponsor: Defense Research and Development Organization (India; through the Defense Research and Development Organization/ISRO–Pune University Interaction Cells).

The first approach involves the synthesis of substituted conducting polymer coatings on oxidizable metals to explore the possibility of using them as alternatives to their parent polymers for corrosion protection. We have developed appropriate electrochemical polymerization procedures to synthesize strongly adherent poly(*o*-anisidine),[29,30] poly(*o*-toluidine) (POT),[31,32] poly(2,5-dimethoxyaniline),[33] and poly(2,5-dimethylaniline)[34] coatings on substrates of low-carbon steel (LCS) and copper (Cu). These coatings have a remarkable ability to protect LCS and Cu against corrosion.

The second approach involves the formation of bilayer coatings that consist either of a top coat of a conducting polymer on the layer of another conducting polymer or a top layer of a conducting polymer on a metallic coating such as nickel. Recently, Tuken and his research group[35–38] extensively studied the electrochemical synthesis of PANI and polypyrrole coatings on nickel-plated mild steel and Cu substrates from aqueous media. They investigated the corrosion behavior of these coatings through immersion tests performed in different corrosive media and recorded electrochemical impedance spectra at different exposure times.

The third approach involves the use of copolymerization to prepare new polymers with inbuilt, tailor-made properties suitable for the application. Recently, Bereket et al.[39] reported the electrochemical synthesis of poly(aniline-*co*-2-anisidine) films on stainless steel in a tetrabutylammonium perchlorate/acetonitrile solution containing perchloric acid. They investigated the corrosion properties of these copolymer coatings in a 0.5*M* hydrochloric acid (HCl) solution by a potentiodynamic technique, open-circuit-potential measurements, and electrochemical impedance spectroscopy. They found that PANI, poly (2-anisidine), and poly(aniline-*co*-2-anisidine) films have a corrosion-protection effect for 304 stainless steel in an aggressive medium of a 0.5 HCl solution. However, the durability of the poly(aniline-2-anisidine) films is limited to 3 h.

In the work reported in this article, we have attempted to synthesize strongly adherent poly(aniline-*co*-*o*-toluidine) (PAOT) coatings on LCS substrates from aqueous media with cyclic voltammetry and evaluated the performance of these copolymer coatings against the corrosion of steel in aqueous 3% NaCl. To the best of our knowledge, there are no reports in the literature dealing with the direct deposition of PAOT coatings on LCS from aqueous media.

The objectives of this study are (1) to report new findings on the electrochemical copolymerization of aniline with *o*-toluidine on LCS from aqueous media; (2) to find a potentially good, low-cost, and easily available electrolyte for the electrochemical synthesis of strongly adherent PAOT coatings on LCS substrates; (3) to characterize these coatings with electrochemical and spectroscopic techniques; and (4) to evaluate the performance of these copolymer coatings against the corrosion of steel in aqueous 3% NaCl.

Recently, we have shown that the electrochemical polymerization of *o*-anisidine in an aqueous tartrate solution results in the deposition of uniform and strongly adherent poly(*o*-anisidine) coatings on LCS substrates.[30] These coatings exhibit excellent corrosion-protection properties, and poly(*o*-anisidine) has been found to be the most promising coating material for the corrosion protection of LCS in aqueous 3% NaCl. In view of its ability to passivate the LCS substrate without preventing monomer oxidation, sodium tartrate was chosen as the supporting electrolyte for the electrochemical copolymerization of aniline with *o*-toluidine on LCS.

EXPERIMENTAL

Materials

The monomers, aniline and *o*-toluidine, were doubly distilled before being used for the synthesis of the homopolymer and copolymer coatings. In this study, an aqueous sodium tartrate solution was used as the supporting electrolyte.

The chemical composition (by wt %) of the LCS used in this study was 0.03% C, 0.026% S, 0.01% P, 0.002% Si, 0.04% Ni, 0.002% Mo, 0.16% Mn, 0.093% Cu, and 99.64% Fe. The LCS substrates ($\sim 10 \times 15 \times 0.5$ mm^3) were polished with a series of emery papers, and this was followed by thorough rinsing in acetone and double-distilled water and drying in air. Before any experiment, the substrates were treated as described and freshly used with no further storage.

Synthesis of the PANI, POT, and PAOT copolymer coatings

The PANI, POT, and PAOT copolymer coatings were synthesized on LCS substrates with cyclic voltammetry. To synthesize the PANI and POT homopolymer coatings, the concentrations of the respective monomer and the sodium tartrate were kept constant at 0.2*M* each. For the electrochemical copolymerization, a mixture of aniline and *o*-toluidine with a total concentration of 0.2*M* was used in a 0.2*M* aqueous tartrate solution. We carried out the copolymer synthesis experiments with *o*-toluidine feed ratios of 0.1, 0.3, 0.5, 0.7, and 0.9 by taking *o*-toluidine/(aniline + *o*-toluidine) ratios of 10 : 90, 30 : 70, 50 : 50, 70 : 30, and 90 : 10, respectively. we abbreviated the synthesized copolymer coatings by taking into considera-

tion the *o*-toluidine feed ratio used for the synthesis. For example, the copolymer coating synthesized with an *o*-toluidine feed ratio of 0.5 was abbreviated PAOT5.

The electrochemical polymerization was carried out in a single-compartment, three-electrode cell with LCS as the working electrode (1.5 cm^2), platinum as the counter electrode, and a saturated calomel electrode (SCE) as the reference electrode. The cyclic voltammetry conditions were maintained with a Parstat 2363-1 (EG and G, Princeton Applied Research, Princeton, NJ) controlled by PerkinElmer Instruments 2000 PowerSuite software (supplied by EG and G, Princeton Applied Research). The synthesis was carried out by continuous cycling of the electrode potential between −500 and 1500 mV at a potential scanning rate of 20 mV/s. After 10 cycles, the working electrode was removed from the electrolyte, rinsed with double-distilled water, and dried in air.

Characterization of the coatings

The PANI, POT, and PAOT coatings were characterized with cyclic voltammetry, ultraviolet–visible (UV–vis) absorption spectroscopy, Fourier transform infrared (FTIR) spectroscopy, nuclear magnetic resonance (NMR) spectroscopy, and scanning electron microscopy (SEM). The FTIR transmission spectra of the homopolymer and copolymer coatings were recorded in a horizontally attenuated total reflectance mode in the spectral range of 4000–400 cm^{-1} with a PerkinElmer 1600 series II spectrometer. The UV–vis absorption spectroscopy study was carried out *ex situ* in the wavelength range of 300–1100 nm with a microprocessor-controlled, double-beam UV–vis spectrophotometer (model U 2000, Hitachi, Tokyo, Japan). SEM was employed to characterize the surface morphology with a Leica (United Kingdom) Cambridge 440 microscope. The ^{1}H-NMR spectra were obtained on a Bruker DSX-300 solid-state NMR spectrometer operating at 300 MHz. The measurements were carried out in dimethyl sulfoxide-d_6 (DMSO-d_6) solutions at the ambient temperature.

Study of the corrosion-protection performance of the coatings

The corrosion-protection performance study was performed at room temperature in aqueous solutions of 3% NaCl with open-circuit-potential measurements and a potentiodynamic polarization technique. For these measurements, a Teflon holder was used to encase the polymer-coated LCS substrates so as to leave an area of $\sim$ 0.4 cm^2 exposed to the solution. The polarization resistance measurements were performed by the potential being swept between −250 and 250 mV from the open circuit potential at a scanning rate of 2 mV/s.[40] Before polarization, the substrates were immersed into the solution, and the open circuit potential was monitored until a constant value was reached. The Tafel slopes of the anodic (β_a) and cathodic (β_b) parts of the polarization curve were obtained. The corrosion current density [I_{corr} (A/cm^2)] was calculated with the Stern–Geary equation[41] and was converted into the corrosion rate (CR) in millimeters per year as follows[42]:

$$CR(mm/yr) = 3.268 \times 10^3 I_{corr} \frac{EW}{\rho}$$

where EW is the equivalent weight of LCS (g) and ρ is the density of LCS (g/cm^3). All the measurements were repeated at least four times, and good reproducibility of the results was observed.

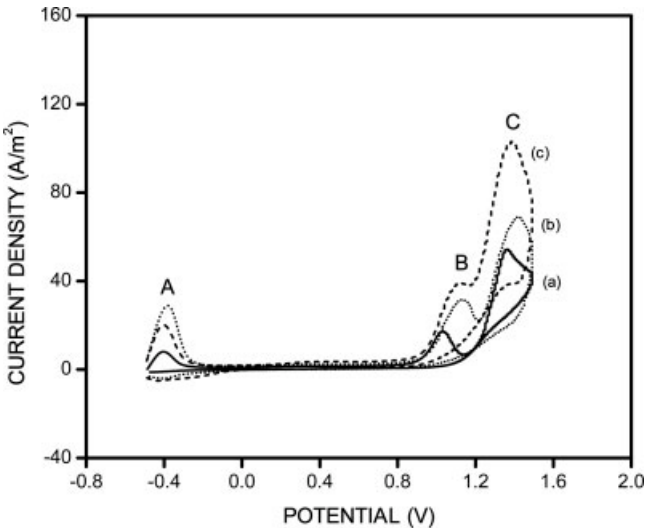

Figure 1 Cyclic voltammograms of the first scans recorded during the syntheses of (a) PANI, (b) POT, and (c) PAOT5 copolymer coatings on LCS substrates.

RESULTS AND DISCUSSION

Electrochemical synthesis of the PANI and POT homopolymer and PAOT copolymer coatings on LCS

The cyclic voltammograms of the first scans recorded during the syntheses of the PANI and POT homopolymer and PAOT5 copolymer coatings on the LCS substrate from aqueous tartrate solutions are shown in Figure 1. The first positive cycle of these voltammograms is characterized by three anodic peaks (A, B, and C). During the reverse cycle, the anodic current density decreases rapidly, and a negligibly small current density can be seen till the end of the cycle. These cyclic voltammograms are qualitatively similar to those reported by Wankhede et al.,[30] who

investigated the electrochemical polymerization of *o*-anisidine on LCS in aqueous tartrate solutions.

Anodic peak A is attributed to the dissolution of the LCS electrode surface. In the potential range of −500 to −207 mV, the LCS electrode is reactive and undergoes anodic dissolution, which produces Fe^{2+} ions in its vicinity. These ions interact with the tartrate counterions of the electrolyte to form insoluble iron(II) tartrate ($FeC_4H_4O_6$), which adheres to the electrode surface, thereby forming an iron tartrate film. This interphase is produced according to the following two reactions[30]:

$$Fe \rightarrow Fe^{2+} + 2e^-$$

$$Fe^{2+} + (C_4H_4O_6)^{2-} \rightarrow FeC_4H_4O_6$$

Oxidation peak B corresponds to the oxidation of the monomer(s) and formation of radical cations, which are rapidly consumed in subsequent reactions to yield dimers, trimers, tetramers, and so forth. Anodic peak C is assigned to the oxidation of the tartrate electrolyte.

A careful examination of these cyclic voltammograms leads to the following conclusions. First, the area of anodic peak A differs significantly, depending on the monomer(s) present in the electrolyte, and it follows the order of *o*-toluidine > (aniline + *o*-toluidine) > aniline.

As discussed earlier, anodic peak A is related to the passivation process of the LCS substrate. During this process, the dissolution of the electrode surface takes place, and the passive interphase is formed on the electrode surface. Because of this process, a certain charge is required to start the electrochemical polymerization process. The amount of the passivation charge depends on the experimental conditions employed, such as the nature of the substrate, the supporting electrolyte, the solvent, the pH of the electrolyte, the synthesis temperature, and the applied current density. It is thought that the monomer (e.g., aniline or *o*-toluidine) present in the electrolyte solution does not influence the passivation process. Obviously, it is expected that the passivation charge required to start the electrochemical polymerization process of the conducting polymer under identical experimental conditions should be the same, regardless of the type of monomer present in the electrolyte solution. However, the experimental results show that the area of anodic peak A differs significantly, depending on the monomer(s) present in the electrolyte. This suggests that the type of monomer present in the electrolyte solution affects the passivation process of the LCS electrode. Moreover, when the feed concentration of *o*-toluidine in the comonomer feed is varied, the area of peak A shows systematic variation. The variation of the area of peak A as a function of the concentration of *o*-toluidine in the comonomer feed is shown in Figure 2. The area of peak A decreases with the decrease in the concentration of *o*-toluidine in the comonomer feed. *o*-Toluidine is a substituted derivative of aniline with an electron-donating methyl (—CH_3) group substituted at the ortho position. Thus, *o*-toluidine is more reactive than aniline in electrophilic substitution reactions because of the electron-donating effect.[43] Therefore, the results of the cyclic voltammetry may be attributed to the reactivity of *o*-toluidine being higher than that of aniline during the electrochemical copolymerization of aniline with *o*-toluidine.

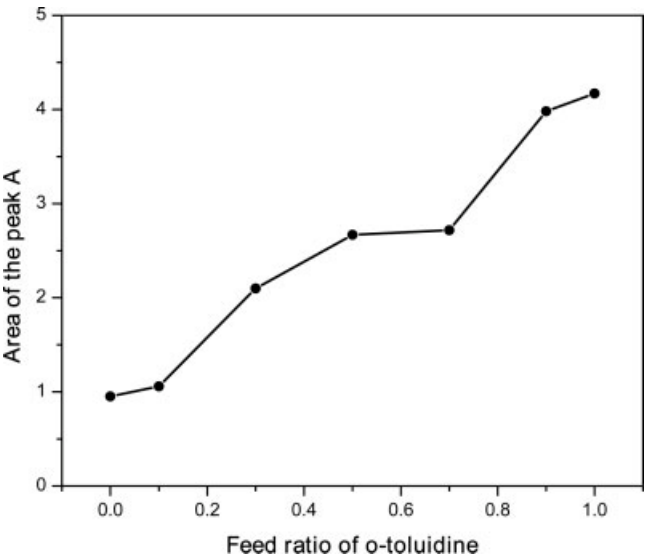

Figure 2 Variation of the area of peak A as a function of the feed ratio of *o*-toluidine.

Second, the current density of oxidation peak B of the combined monomers (aniline and *o*-toluidine) is higher than the oxidation current density of the respective individual monomers aniline and *o*-toluidine. This suggests that aniline and *o*-toluidine are simultaneously oxidized to generate the respective cation radicals. There can be two possibilities for further reactions. First, these cation radicals undergo self-polymerization, which results in the formation of respective homopolymers, that is, PANI and POT. In such a case, the subsequent scans of the cyclic voltammogram recorded during the electrochemical copolymerization of aniline and *o*-toluidine should bear a resemblance to the voltammogram scans of the homopolymers, PANI and POT. On the other hand, the reactivities of the generated cation radicals favor a cross reaction between them, which would result in a new intermediate consisting of aniline and *o*-toluidine units. In such a case, the cyclic voltammograms of the subsequent scans recorded during the electrochemical copolymerization of aniline and *o*-toluidine should be different than the

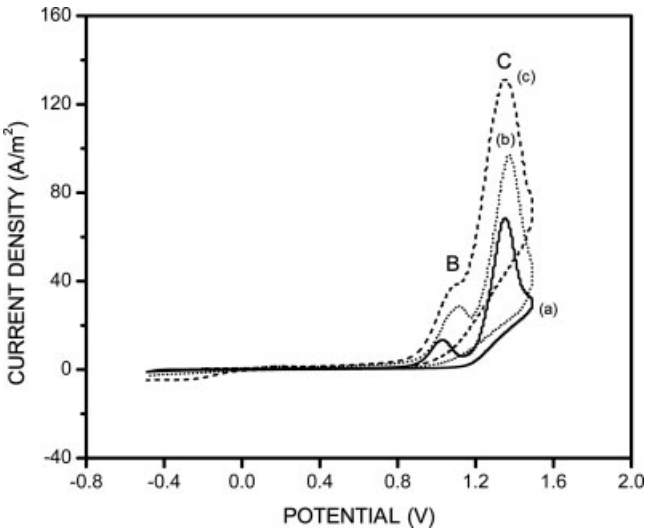

Figure 3 Cyclic voltammograms of the second scans recorded during the syntheses of (a) PANI, (b) POT, and (c) PAOT5 copolymer coatings on LCS substrates.

voltammograms observed for the formation of the homopolymers, that is, PANI and POT.

The cyclic voltammograms of the second scans recorded during the syntheses of the PANI and POT homopolymer and PAOT5 copolymer coatings on the LCS substrate from aqueous tartrate solutions are shown in Figure 3. These voltammograms indicate that anodic peak A, corresponding to the dissolution of LCS, cannot be observed, but the rest of the characteristics are similar to those of the first scan. Moreover, the current densities corresponding to the oxidation peaks increase during the second scan, and this indicates the growth of the conducting polymer coating. The cyclic voltammogram of the second scan [Fig. 3(c)] recorded during the electrochemical copolymerization of aniline with *o*-toluidine is qualitatively similar to those obtained for the individual homopolymerization. However, the current densities corresponding to anodic peaks B and C are considerably higher than those observed during the individual homopolymerization. These observations strongly suggest that the electrochemical copolymerization of aniline with *o*-toluidine on LCS in an aqueous tartrate solution generates true copolymer coatings rather than a mixture of the corresponding homopolymers.

Voltammograms of the subsequent scans identical to those of the second scan were obtained up to the third scan. After the third scan, the current density corresponding to the anodic peaks decreases gradually with the number of scans, and the cyclic voltammograms do not show well-defined redox peaks. A typical cyclic voltammogram of the tenth scan recorded during the syntheses of PANI, POT, and PAOT5 coatings on the LCS substrate are shown in Figure 4.

The FTIR spectra of the PANI and POT homopolymer and PAOT5 copolymer coatings on LCS are shown in Figure 5. The characteristic bands in the FTIR spectrum of PANI [Fig. 5(a)] are assigned as follows[44–47]: the broad band at ~3354 cm^{-1} is due to the N—H stretching mode, the C=N and C=C stretching mode for the quinoid and benzoid rings occurs at 1596 and 1511 cm^{-1}, the band at ~ 1303 cm^{-1} can be assigned to the C—N stretching mode for benzoid rings, and the bands between 800 and 700 cm^{-1} reveal the occurrence of 1–3-substitutions.

The FTIR spectrum of POT [Fig. 5(b)] is similar to the spectrum of PANI, except for a band that appears at ~ 1111 cm^{-1}. This band is attributed to the —CH_3 rocking mode.

The FTIR spectrum of the PAOT5 copolymer coating on LCS [Fig. 5(c)] is presented in Figure 5(c). The most striking feature of the spectrum of PAOT5 is that it exhibits a greater similarity to the spectrum of POT. Moreover, the intensity of the band at ~ 1111 cm^{-1} corresponding to the —CH_3 rocking mode increases as the amount of *o*-toluidine in the comonomer feed increases. These observations indicate a high number of the *o*-toluidine units in the composition of PAOT5. This shows qualitatively a higher reactivity for *o*-toluidine than for aniline in the electrochemical copolymerization.

To establish that PAOT5 is a copolymer rather than a mixture of homopolymers PANI and POT, these polymers were further characterized with ^{1}H-NMR spectroscopy. The ^{1}H-NMR spectra of PANI, POT, and PAOT5, recorded in DMSO-d_6, are shown in Figure 6. The ^{1}H-NMR spectrum of POT [Fig. 6(a)] is characterized by the presence of three main signals.[43,48] The signals in the region of 6.8–7.4 ppm are

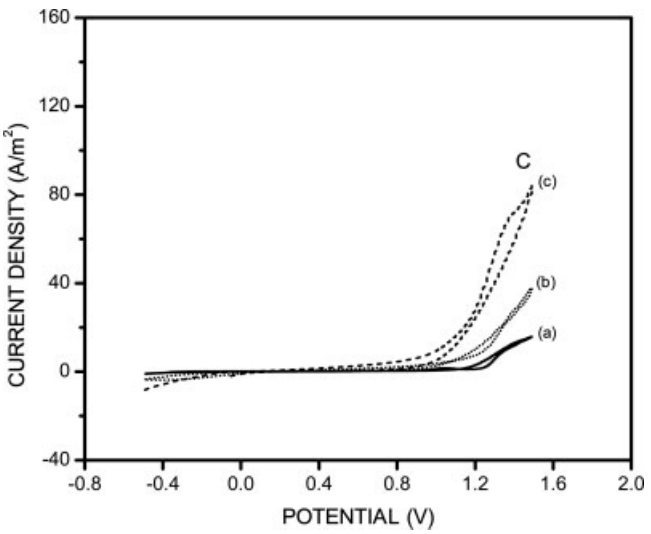

Figure 4 Cyclic voltammograms of the tenth scans recorded during the syntheses of (a) PANI, (b) POT, and (c) PAOT5 copolymer coatings on LCS substrates.

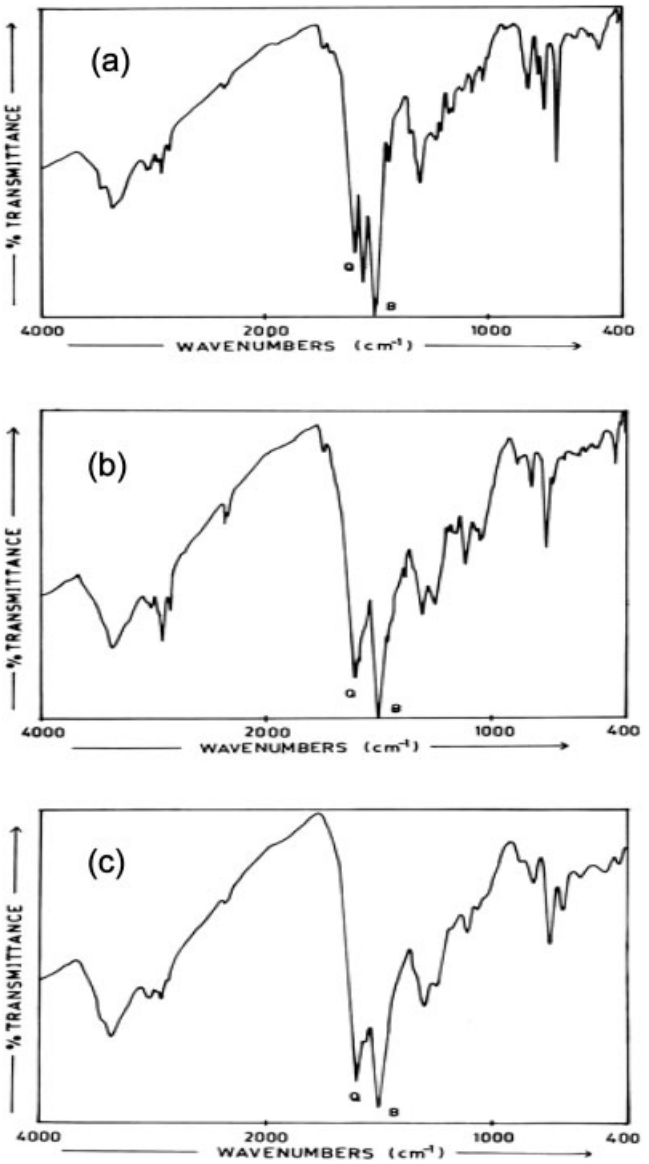

Figure 5 FTIR spectra of (a) PANI, (b) POT, and (c) PAOT5 copolymer coatings synthesized on LCS substrates with cyclic voltammetry.

due to the protons of the aromatic rings. The resonances in the region of 1.8–2.1 ppm are attributed to the methyl protons of the quinoid ring, and those in the region of 1.1–1.3 ppm are due to the methyl protons of the benzoid ring. The ^{1}H-NMR spectrum of PANI [Fig. 6(b)] shows the presence of signals in the region of 6.5–7.8 ppm, which are assigned to the protons of the aromatic rings. The spectrum of PANI does not show the signal in the region of 1.8–2.1 ppm corresponding to the methyl protons.

The ^{1}H-NMR spectrum of the PAOT5 copolymer [Fig. 6(c)] has essentially the same characteristics as that of POT. This spectrum is characterized by three main signals that exactly correspond to the three types of protons on the copolymer chains. As can be seen in Figure 6(c), this spectrum exhibits the signals in a wide range from 6.2 to 7.8 ppm, which are attributed to the aromatic protons on the aniline and *o*-toluidine units. The resonance peaks from 1.92 and 2.20 ppm are assigned to the protons of the methyl groups on the quinoid ring. The two strongest peaks at 2.39 and 3.28 ppm are due to protons of dimethyl sulfoxide (DMSO) and water in DMSO, respectively. Additionally, two negligibly small signals at 5.2 and 5.8 ppm are assigned to the —NH— linkages. This indicates the formation of a high-molecular-weight PAOT5 copolymer. The actual *o*-toluidine/aniline ratio in the copolymer can be approximately calculated from the area ratio of the *o*-toluidine aromatic proton peak to the aniline aromatic proton peak. The actual *o*-toluidine/aniline molar ratio calculated by this method is ~1.6 for the PAOT5 copolymer. This suggests that in the resulting copolymer, there are more *o*-toluidine units than aniline units. This supports a higher reactivity of *o*-toluidine versus aniline in the copolymerization and is reflected in the cyclic voltammetry and FTIR spectroscopy results. This observation is in agreement with the results reported by Wei et al.[48] These authors synthesized PAOT and

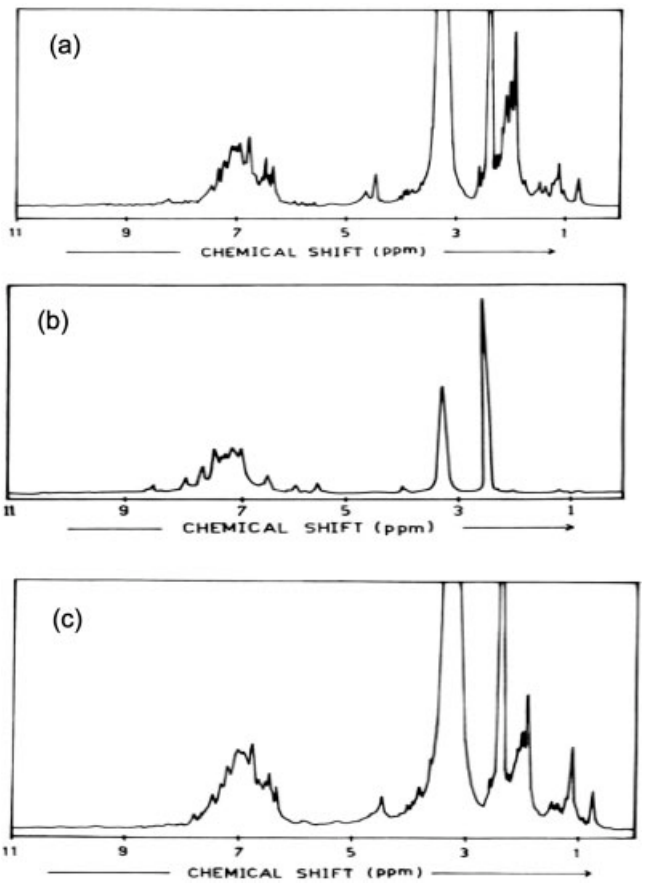

Figure 6 ^{1}H-NMR spectra of (a) PANI, (b) POT, and (c) PAOT5 recorded in DMSO-d_6 at 300 MHz.

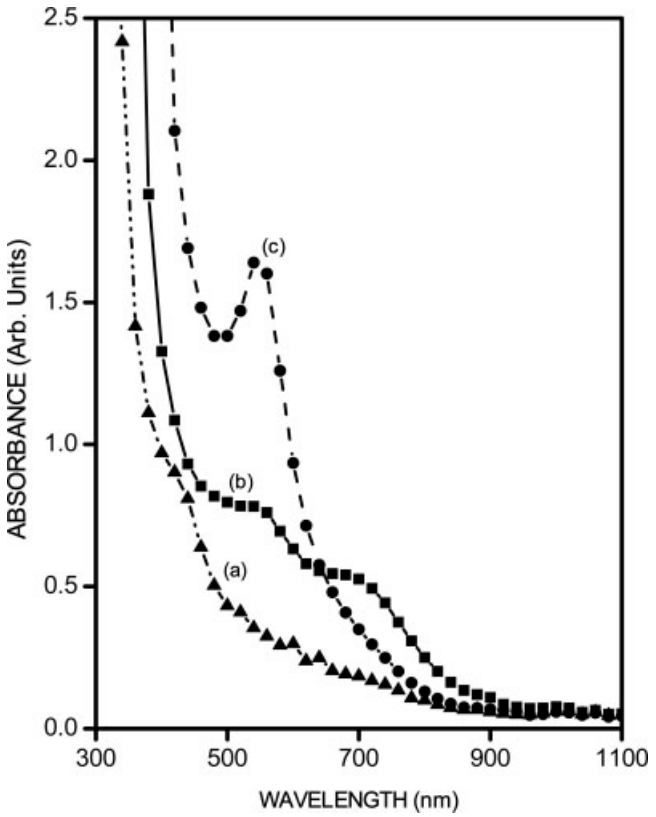

Figure 7 Optical absorption spectra of (a) PANI, (b) POT, and (c) PAOT5 copolymer coatings synthesized on LCS with cyclic voltammetry (the spectra were recorded *ex situ* in DMSO solutions).

poly(aniline-*co*-*m*-toluidine) copolymers by chemical polymerization with sodium persulfate as an oxidant in aqueous 1*M* HCl solutions. They reported that *o*-toluidine had higher reactivity than aniline in the copolymerization process. Thus, the ^{1}H-NMR spectroscopy study confirms that aniline and *o*-toluidine are indeed able to copolymerize on LCS in an aqueous tartrate medium, and in the resulting PAOT5 copolymer, there are more *o*-toluidine units than aniline units.

The optical absorption spectra of the PANI and POT homopolymer and PAOT5 copolymer coatings are shown in Figure 7. The spectral characteristics of the PAOT5 copolymer are remarkably different from those of the individual homopolymers PANI and POT.

The optical absorption spectrum of the PANI coating synthesized on LCS [Fig. 7(a)] shows a high value of the absorbance between 600 and 800 nm with a weak shoulder at ~740 nm. This shoulder peak at 740 nm is attributed to the formation of the emeraldine salt (ES) form of PANI in the coating.[49] The higher value of the absorbance between 600 and 740 nm may be due to the formation of some species with other oxidation states. Thus, the optical absorption spectroscopy reveals the formation of the ES form along with some other oxidation-state species.

The optical absorption spectrum of the POT coating [Fig. 7(b)] shows broad peaks at about 560 and 720 nm. The peak at 560 nm is attributed to the presence of the pernigraniline base (PB) form of POT. PB is the fully oxidized form of POT and is insulating in nature.[49] The shoulder at ~ 720 nm is a signature of the ES form of POT. The simultaneous appearance of 540 and 720 nm reveals the formation of a mixed phase of PB and ES forms of POT.

The optical absorption spectrum of the PAOT5 copolymer coating [Fig. 7(c)] shows a well-defined peak at ~ 540 nm, and it is attributed to the formation of the PB form of PAOT5.

The surface morphologies of PANI and POT homopolymer and PAOT5 copolymer coatings synthesized on LCS were characterized with SEM. The surface morphology of the PANI coating [Fig. 8(a)] is rough and is characterized by the presence of pores in the coating. The surface morphology of the POT coating [Fig. 8(b)] is relatively uniform and featureless. The SEM image of the copolymer PAOT5 coating synthesized on LCS is shown in Figure 8(c). It clearly reveals that the copolymer PAOT5 coating is relatively uniform, featureless, and pore-free.

Corrosion-protection performance of the PAOT copolymer coating

The open-circuit-potential/time curves recorded in aqueous 3% NaCl for PANI-, POT-, and PAOT5-coated LCS are presented in Figure 9. In this figure, −710 mV stands for the corrosion potential (E_{corr}) of uncoated LCS. The initial open-circuit-potential values measured for PANI-, POT-, and PAOT5-coated LCS are −420, −349, and −333 mV versus SCE and are more positive than that of uncoated steel. In the early stages of the immersion, the open circuit potential in each case decreases rapidly, and this may be due to the initiation of the water uptake process through the pores in the coating toward the substrate surface. However, these values are more positive than that of uncoated steel.

The open circuit potential of PAOT5-coated LCS remains almost constant for longer periods (~ 30 h), and its potential value is more noble with respect to the open-circuit value of the uncoated LCS and homopolymer-coated LCS. During this immersion period, the PAOT5 coating exhibits barrier behavior by limiting the diffusion of the corrosive species toward the underlying steel substrate. This behavior is attributed to the corrosion-protection effect for the LCS caused by the PAOT5 copolymer coating.

The porosity in the coating strongly governs the anticorrosive behavior of the coatings; therefore, the determination of the porosity in the coating is essen-

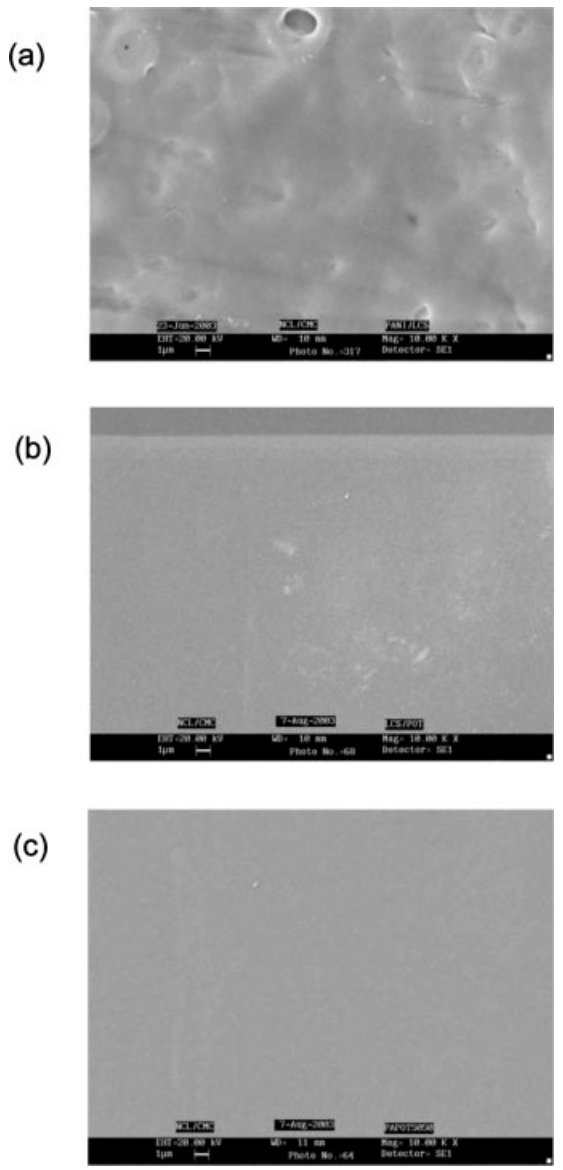

Figure 8 SEM images of LCS coated with (a) PANI, (b) POT, and (c) PAOT5.

tial to estimate the overall corrosion resistance of the coated substrate. The porosity in PANI, POT, and PAOT5 coatings on LCS substrates was determined from potentiodynamic polarization measurements. The potentiodynamic polarization curve of uncoated LCS recorded in aqueous 3% NaCl is shown in Figure 10, and the curves for PANI-coated LCS, POT-coated LCS, and PAOT5-coated LCS (10 cycles) are shown in Figure 11. The values of E_{corr}, I_{corr}, Tafel constants β_a and β_c, the polarization resistance (R_p), and CR obtained from these curves are given in Table I. The porosity of the coatings was calculated with the following relation:[50]

$$P = \frac{R_{ps}}{R_{pc}} 10^{-\left(\frac{|\Delta E_{corr}|}{\beta_a}\right)}$$

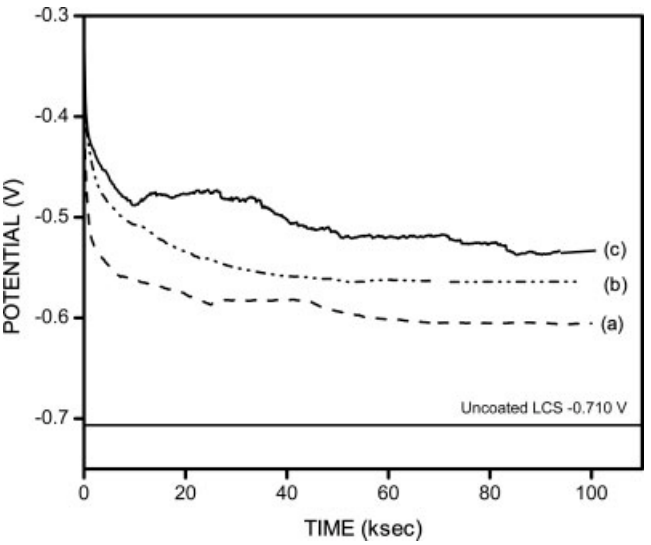

Figure 9 Open-circuit-potential/time curve recorded for (a) PANI-coated LCS, (b) POT-coated LCS, and (c) PAOT5-coated LCS in aqueous 3% NaCl. The continuous line represents the open circuit potential of uncoated LCS.

where P is the total porosity, R_{ps} is the polarization resistance of bare LCS, R_{pc} is the measured polarization resistance of coated LCS, ΔE_{corr} is the difference between the corrosion potentials, and β_a is the anodic Tafel slope for the bare LCS substrate. The

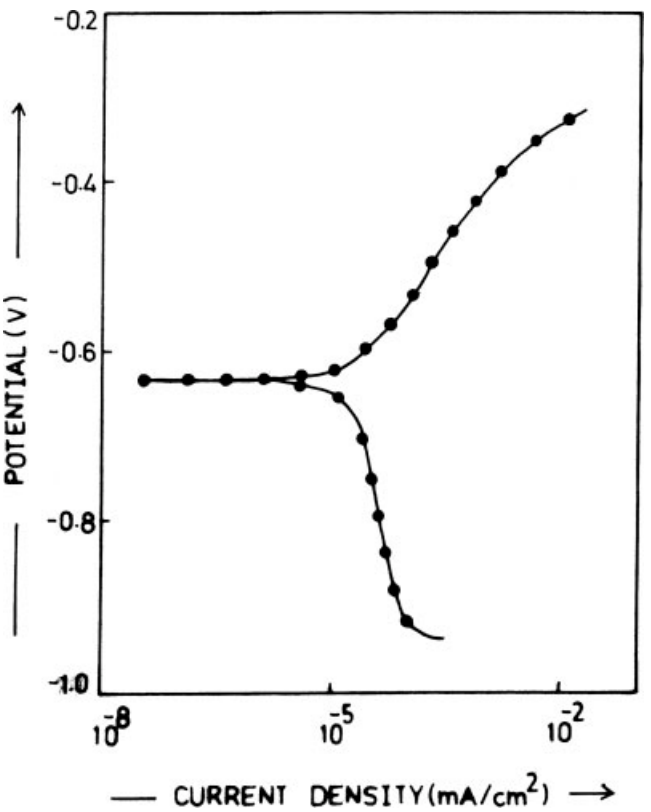

Figure 10 Potentiodynamic polarization curves for uncoated LCS recorded in aqueous 3% NaCl solutions.

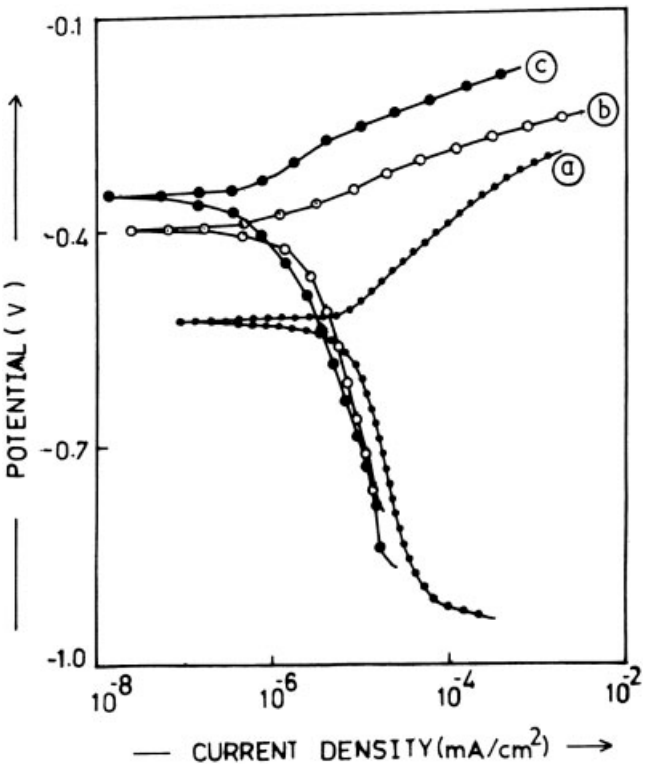

Figure 11 Potentiodynamic polarization curves for (a) PANI-coated LCS, (b) POT-coated LCS, and (c) PAOT5-coated LCS recorded in aqueous 3% NaCl solutions.

porosity in the PANI, POT, and PAOT5 copolymer coatings was found to be $\sim 1.7 \times 10^{-1}$, 3.0×10^{-3}, and 2.0×10^{-4} %, respectively. The significantly lower values of the porosity in the PAOT5 copolymer coatings versus those of the respective homopolymer coatings permit substantial improvement of the corrosion resistance by hindering the access of the electrolyte to the stainless steel substrates.

An analysis of these potentiodynamic polarization curves shows a positive shift in E_{corr} and a substantial reduction in I_{corr} of LCS due to the PANI, POT, and PAOT5coatings, and this indicates the corrosion-resistant character of PANI, POT, and PAOT5. The shift in E_{corr} depends on the coating and decreases in the order of PAOT5 > POT > PANI. This implies that the PAOT5 copolymer coating provides effective protection for LCS against corrosion in aqueous 3% NaCl in comparison with those of the corresponding homopolymers.

I_{corr} decreases from 17.79 μA/cm^2 for uncoated LCS to 6.26, 1.50, and 0.41 μA/cm^2 for PANI-, POT-, and PAOT5-coated LCS, respectively. The CR values of PANI-, POT-, and PAOT5-coated LCS are $\sim$ 0.07, 0.01, and 0.004 mm/year, which are $\sim$ 3, 20, and 50 times lower than that observed for uncoated LCS. The protection efficiency (PE) was calculated as follows:

$$\text{PE\%} = \left[\frac{R_{pc} - R_p}{R_{pc}}\right] \times 100$$

where R_p is the polarization resistance of uncoated LCS. The PEs for PANI, POT, and the PAOT5 copolymer calculated from potentiodynamic polarization data are $\sim$ 69, 85, and 96%, respectively. These results reveal that the PAOT5 copolymer effectively protects LCS and improves the corrosion PE with respect to that offered by the corresponding homopolymers.

To investigate the influence of the *o*-toluidine concentration in the comonomer feed on the corrosion-protection properties of the PAOT copolymer coatings, we synthesized coatings with *o*-toluidine feed ratios of 0.1, 0.3, 0.5, 0.7, and 0.9, and the potentiodynamic polarization measurements were performed in aqueous 3% NaCl solutions. The dependence of the positive shift in E_{corr} (ΔE_{corr}) on the feed ratio of *o*-toluidine is shown in Figure 12. ΔE_{corr} increases with the feed ratio of *o*-toluidine and attains a maximum value of 386 mV at a 0.5 feed ratio. With a further increase in the feed ratio of *o*-toluidine to 0.7, ΔE_{corr} decreases to 334 mV, and beyond this, it does not show any significant variation in ΔE_{corr}.

The variation of the CR as a function of the feed ratio of *o*-toluidine is also shown in Figure 12. The initial value of CR decreases significantly when the feed ratio of *o*-toluidine increases and is lowest ($\sim$ 50 times lower than that of uncoated LCS) for the feed ratio of 0.5. With a further increase in the feed

TABLE I
Results of the Potentiodynamic Polarization Measurements

Sample	E_{corr} (mV)	I_{corr} (μA/cm^2)	β_a (mV/dec)	β_c (mV/dec)	R_p (Ω/cm^2)	CR (mm/yr)	P (%)
Bare LCS	−710	17.79	91.20	270.38	1,664.57	0.20	—
PANI	−506	6.26	95.94	438.47	5,456.94	0.07	0.17
POT	−375	1.49	43.81	342.34	11,281.28	0.01	0.003
PAOT1	−512	2.74	110.0	297.73	12,743.40	0.03	0.088
PAOT3	−402	0.686	77.05	330.25	39,534.10	0.007	0.001
PAOT5	−329	0.4187	47.61	231.81	40,963.77	0.004	0.0002
PAOT7	−376	0.486	61.79	260.45	44,579.41	0.005	0.0008
PAOT9	−368	0.6292	120.5	277.01	57,953.11	0.007	0.0005

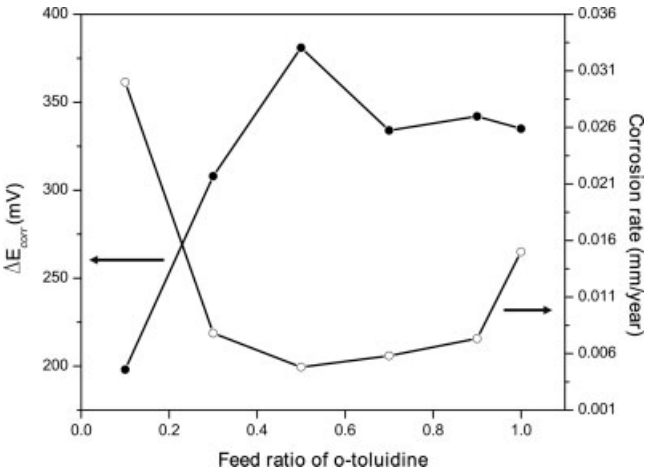

Figure 12 Dependence of ΔE_{corr} and CR on the feed ratio of *o*-toluidine.

ratio of *o*-toluidine, CR increases slowly, and with a feed ratio of 1, CR is 0.015 mm/yr. Thus, more effective protection of LCS against corrosion in 3% NaCl can be achieved by the copolymer coatings synthesized with a feed ratio of *o*-toluidine of 0.5.

CONCLUSIONS

Strongly adherent PAOT coatings were successfully synthesized on LCS substrates from aqueous tartrate solutions with cyclic voltammetry. The performance of the PAOT coatings as protective coatings against the corrosion of LCS in aqueous 3% NaCl solutions was investigated with open-circuit-potential measurements and a potentiodynamic polarization technique. The following main findings resulted from this investigation:

- The results clearly show that an aqueous sodium tartrate solution is a suitable medium for the electrochemical copolymerization of aniline with *o*-toluidine on LCS.
- The FTIR and ^{1}H-NMR spectroscopy studies reveal that the copolymerization of aniline and *o*-toluidine takes place on LCS in aqueous tartrate solutions, and in the resulting PAOT copolymer, there are more *o*-toluidine units than aniline units.
- The porosity in the coating has been estimated with the potentiodynamic polarization measurements, and the porosity values are significantly lower for the PAOT coatings than for the respective homopolymers, that is, PANI and POT. The copolymer coatings are more compact and strongly adherent to LCS.
- The potentiodynamic polarization and open-circuit measurements reveal that the PAOT coatings effectively protect LCS and have higher corrosion PEs than those offered by the corresponding homopolymers.
- The protection of LCS against corrosion in 3% NaCl by the copolymer coatings can be achieved more effectively when the synthesis is carried out with a feed ratio of *o*-toluidine of 0.5.

The authors gratefully acknowledge the NMR Research Center of the Indian Institute of Science (Bangalore, India) for its help in recording the NMR spectra.

References

1. Cai, Z. J.; Geng, M. M.; Tang, Z. Y. J Mater Sci 2004, 39, 4001.
2. Karami, H.; Mousavi, M. F.; Shamsipur, M. J Power Sources 2003, 117, 255.
3. Grennan, K.; Killard, A. J.; Hanson, C. J.; Cafolla, A. A.; Smyth, M. R. Talanta 2006, 68, 1591.
4. Sengupta, P. P.; Barik, S.; Adhikari, B. Mater Manufact Process 2006, 21, 263.
5. Wang, Y. Y.; Jing, X. L. Polym Adv Technol 2005, 16, 344.
6. Jing, X. L.; Wang, Y. Y.; Zhang, B. Y. J Appl Polym Sci 2005, 98, 2149.
7. Morita, M. Makromol Chem 1993, 194, 2361.
8. Srinivasan, S.; Pramanik, P. J Mater Chem 1994, 13, 365.
9. Pineri, M.; Schultze, J. W.; Vorotyntsev, M. A. Electrochim Acta 2000, 45, 2403.
10. Sexena, V.; Malhotra, B. D. Curr Appl Phys 2003, 3, 293.
11. Arulepp, M.; Permann, L. J Power Sources 2004, 133, 320.
12. Mansouri, J.; Burford, R. P. J Membr Sci 1994, 87, 23.
13. Bereket, G.; Hur, E.; Sahin, Y. Prog Org Coat 2005, 54, 63.
14. Herrasti, P.; Ocon, P.; Ibanez, A.; Fatas, E. J Appl Electrochem 2003, 33, 533.
15. Huerta-Vilca, D.; Siefert, B.; Moraes, S. R.; Pantoja, M. F.; Motheo, A. J. Mol Cryst Liq Cryst 2004, 415, 229.
16. Shinde, V.; Sainkar, S. R.; Patil, P. P. Corros Sci 2005, 47, 1352.
17. Shinde, V.; Sainkar, S. R.; Patil, P. P. J Appl Polym Sci 2005, 96, 685.
18. Zhang, T.; Zeng, C. L. Electrochim Acta 2005, 50, 4721.
19. Sathiyanarayanan, S.; Devi, S.; Venkatachari, G. Prog Org Coat 2006, 56, 114.
20. Mengoli, G.; Munari, M.; Bianco, P.; Misiani, S. J Appl Polym Sci 1981, 26, 4247.
21. Deberry, D. W. J Electrochem Soc 1985, 132, 1022.
22. Popovic, M. M.; Grgur, B. N. Synth Met 2004, 143, 191.
23. Martins, J. I.; Bazzaoui, M.; Reis, T. C.; Bazzaoui, E. A.; Martins, L. I. Synth Met 2002, 129, 221.
24. Bazzaoui, M.; Martins, L. I.; Bazzaoui, E. A.; Martins, T. I. Electrochim Acta 2002, 47, 2953.
25. Moraes, S. R.; Vilca, D. H.; Motheo, A. J. Prog Org Coat 2003, 48, 28.
26. Ogurtsov, N. A.; Pud, A. A.; Kamarchik, P.; Shapoval, G. S. Synth Met 2004, 143, 43.
27. Handbook of Conducting Polymers; Skotheim, T. A., Ed.; Marcel Dekker: New York, 1986; Vols. I and II.
28. Nalwa, H. S. Handbook of Organic Conductive Molecules and Polymers; Wiley: New York, 1997; Vols. 1–4.
29. Patil, S.; Sainkar, S. R.; Patil, P. P. Appl Surf Sci 2004, 225, 204.
30. Wankhede, M. G.; Gangal, S. A.; Sainkar, S. R.; Patil, P. P. Corros Eng Sci Technol 2005, 40, 121.
31. Shinde, V.; Sainkar, S. R.; Patil, P. P. Corros Sci 2005, 47, 1352.
32. Shinde, V.; Sainkar, S. R.; Patil, P. P. J Appl Polym Sci 2005, 96, 685.
33. Patil, V.; Sainkar, S. R.; Patil, P. P. Synth Met 2003, 140, 57.
34. Shinde, V.; Chaudhari, S.; Sainkar, S. R.; Patil, P. P. Mater Chem Phys 2003, 82, 622.

35. Tuken, T.; Ozyilmaz, A. T.; Yazici, B.; Kardas, G.; Erbil, M. Prog Org Coat 2004, 51, 27.
36. Ozyilmaz, A. T.; Kardas, G.; Erbil, M.; Yazici, B. Appl Surf Sci 2005, 242, 97.
37. Tuken, T.; Ozyilmaz, A. T.; Yazici, B.; Erbil, M. Appl Surf Sci 2004, 236, 292.
38. Tuken, T.; Yazici, B.; Erbil, M. Prog Org Coat 2004, 50, 115.
39. Bereket, G.; Hur, E.; Sahin, Y. Prog Org Coat 2005, 54, 63.
40. Fontana, M. G. Corrosion Engineering, 3rd ed.; McGraw-Hill: New York, 1987.
41. Stern, M.; Geary, A. J Electrochem Soc 1957, 104, 56.
42. Electrochemistry and Corrosion—Overview and Techniques; Application Note CORR-4; EG and G, Princeton Applied Research: Princeton, NJ, 1989.
43. Mav, I.; Zigon, M. Polym Bull 2000, 45, 61.
44. Tang, J.; Jing, X.; Wang, B.; Wang, F. Synth Met 1988, 24, 231.
45. Ohsaka, T.; Ohnuki, Y.; Oyama, N.; Katagiri, G.; Kamisako, K. J Electroanal Chem 1984, 161, 399.
46. Zheng, W. Y.; Levon, K.; Taka, T.; Laakso, J.; Osterholm, J. E. Polym J 1996, 28, 412.
47. Neoh, K. G.; Kang, E. T.; Tan, K. L. J Phys Chem 1991, 95, 10151.
48. Wei, Y.; Hariharan, R.; Patel, S. A. Macromolecules 1990, 23, 764.
49. Patil, S. Ph.D. Thesis, North Maharashtra University, 2000.
50. Creus, J.; Mazille, H.; Idrissi, H. Surf Coat Technol 2000, 130, 224.